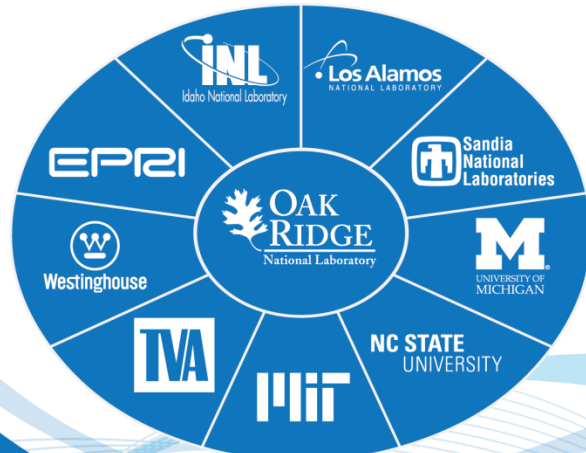


# CASL VMA FY16 Milestone Report (L3:VMA.VUQ.P13.07):<sup>SAND2016-9736R</sup>

## Westinghouse Mixing with COBRA-TF

Natalie Gordon

September 30, 2016



# Problem Impact

Challenge Problem	Code	VVUQ
CIPS ✓	MAMBA-1D	Code Verification
PCI	BISON	Solution Verification
DNB-CTF ✓	CTF ✓	SET Validation
CILC	MPACT	IET Validation ✓
DNB-CFD	MAMBA-3D	Sensitivity
RIA	STAR-1Phase	Uncertainty ✓
LOCA	STAR-2Phase	Calibration ✓

Table 1

Table 1 describes the problem impact of the Hi2Lo work described in the following presentation. The CASL challenge problem benefactors to this work include CIPS and DNB-CTF which use COBRA-TF (CTF). Currently IET Validation and Calibration VVUQ methods are being implemented, and in the future, Uncertainty will also be used.

# OUTLINE

- Introduction
  - Hi2Lo and COBRA-TF (CTF)
  - Westinghouse Provided Experimental Data
    - Geometry used in WEC experiment
    - Parameters provided in WEC experiment report
    - Translation of inlet values from WEC experiment to input parameters needed for CTF
  - Introduction to CTF Hi2Lo phases
- Validation of Training Data
- Calibration of Training Data
  - Non-Bayesian Deterministic Calibration
  - Bayesian Statistical Inference Calibration
- Next Steps
  - CTF output temperature sensitivity to  $\beta$ 
    - Non-Mixing Vane (NMV) bundle outlet temperature sensitivity to  $\beta$  compared to experimental data
    - Mixing Vane (MV) bundle outlet temperature sensitivity to  $\beta$  compared to STAR-CCM+ results and experimental data
  - Axial temperature comparison between CTF and STAR-CCM+

# INTRODUCTION

## Hi2Lo and COBRA-TF (CTF)

COBRA-TF (CTF) is a low-resolution code currently maintained as CASL's subchannel analysis tool. CTF operates as a two-phase, compressible code over a mesh comprised of subchannels and axial discretized nodes. In part because CTF is a low-resolution code, simulation run time is not computationally expensive, only on the order of minutes.

Hi-resolution codes such as STAR-CCM+ can be used to train lower-fidelity codes such as CTF. Unlike STAR-CCM+, CTF has no turbulence model, only a two-phase turbulent mixing coefficient,  $\beta$ .  $\beta$  can be set to a constant value or calculated in terms of Reynolds number using an empirical correlation. Results from STAR-CCM+ can be used to inform the appropriate value of  $\beta$ . Once  $\beta$  is calibrated, CTF runs can be an inexpensive alternative to costly STAR-CCM+ runs for scoping analyses. Based on the results of CTF runs, STAR-CCM+ can be run for specific parameters of interest.

CASL areas of application are CIPS for single phase analysis and DNB-CTF for two-phase analysis.

# INTRODUCTION

## WEC Test Bundle 20 Geometry

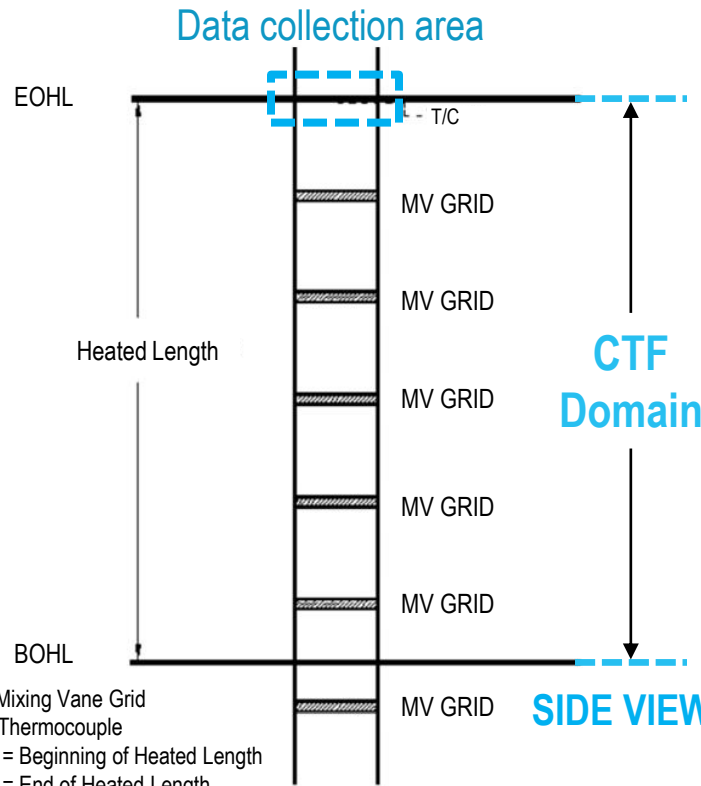


Figure 1

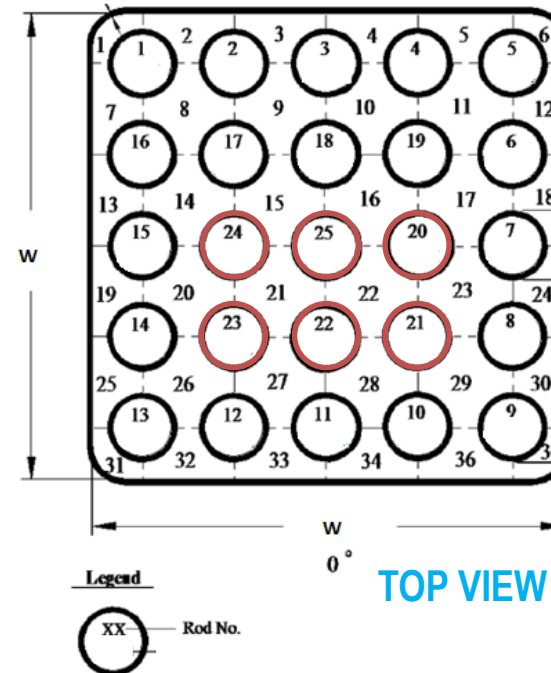


Figure 2

The geometry of Westinghouse (WEC) experimental test bundle 20 consists of a  $5 \times 5$  rod bundle with 5 mixing vane (MV) grids in the heated length. Of the 25 rods, 6 are “hot rods” (pictured in red in Figure 2) with higher power than the other 19 rods. Each of the 36 subchannels shown in Figure 2 contains a thermocouple positioned in the center of the subchannel at the bundle outlet. The data collection area is highlighted by the blue dashed box in Figure 1. The CTF axial domain encompasses the heated length portion of Figure 1 and the mixing vane grids are modeled by loss coefficients applied to the node containing the leading edge of the grid.

# INTRODUCTION

## Westinghouse (WEC) Provided Experimental Data

### Initial Conditions

Test Section Exit Pressure

Test Section Inlet Temperature

Test Section Inlet Enthalpy

Test Section Volumetric Flow Rate

Test Section Mass Velocity

Test Section Power

Test Section Average Heat Flux

Test Section Hot Rod Heat Flux

### Exit Measurements

Average Exit Quality

Exit Temperatures: Subchannels 1-36

Most of the initial condition parameters and exit measurements from the experimental testing are presented on this slide with the rest given in WEC document PFT-16-3. The parameters highlighted in blue are the input and output parameters that are relevant to running CTF. As explained in the next slide, these parameters were converted to those needed for the CTF input decks.

# INTRODUCTION

## Implementation of Westinghouse Experimental Data in CTF

### Initial Conditions

Test Section Exit Pressure (bars)

### CTF Input Parameters

Exit Pressure (psi)

$$\text{Exit Pressure (psi)} = \text{Exit Pressure (bars)} \times 14.50377$$

Test Section Inlet Temperature (°C)

Inlet Temperature (°F)

$$\text{Inlet Temperature (°F)} = \text{Inlet Temperature (°C)} \times 1.8 + 32$$

Test Section Mass Velocity (kg/m<sup>2</sup>-s)

Mass Flow Rate (kg/s)

$$\text{Mass Flow Rate} = \frac{\text{Mass Velocity} \times 2.204623 \times 4.2628}{1550.003}$$

Test Section Power (MW)

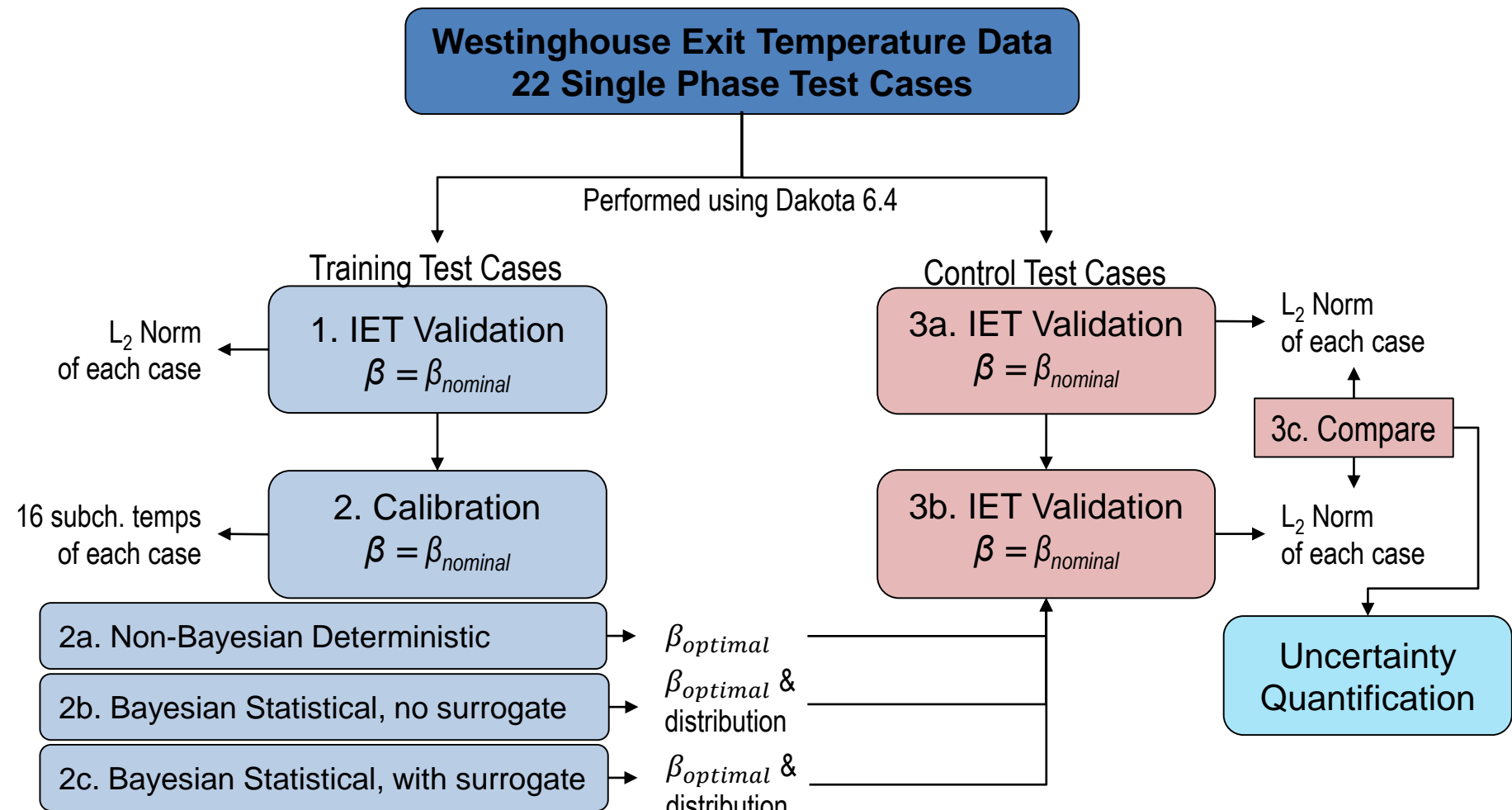
Avg Linear Heat Rate/Rod (kW/ft)

$$AFLUX = \frac{\text{Power} \times 10^3}{25 \times 9.84252}$$

CTF expects different units than those provided in the WEC experimental data. Pressure and temperature were converted from SI units to English units. Mass velocity was converted to mass flow rate using the cross sectional flow area and power was converted to average linear heat rate per rod by dividing by the heated length and number of rods.

# INTRODUCTION

## CTF/Experimental Data Workflow



The 22 test cases were split into training and control data. The training data is used to find the optimal value of  $\beta$  as well as train a surrogate for Bayesian analysis. The control data is used to confirm that the  $\beta$  out of calibration is in fact the optimal  $\beta$ .  $L_2$  norms of outlet temperatures using  $\beta$  nominal and  $\beta$  optimal will be compared to ensure CTF is predicting closer to the experiment than before, followed by Uncertainty Quantification.

# 1. Validation of Training Data

$\beta$  nominal

MV Bundle 20

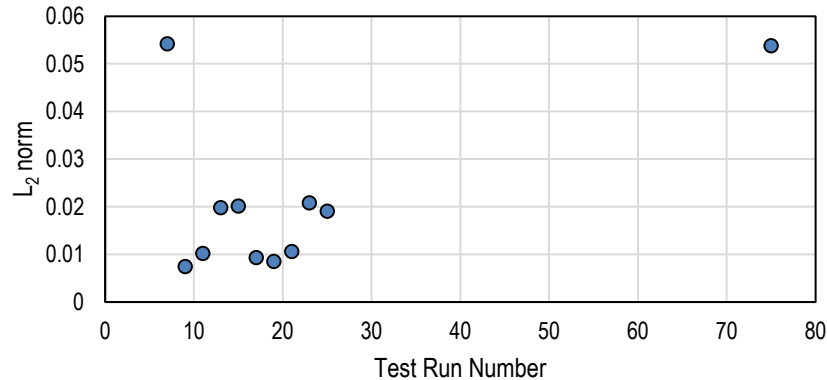


Figure 3

MV Bundle 20

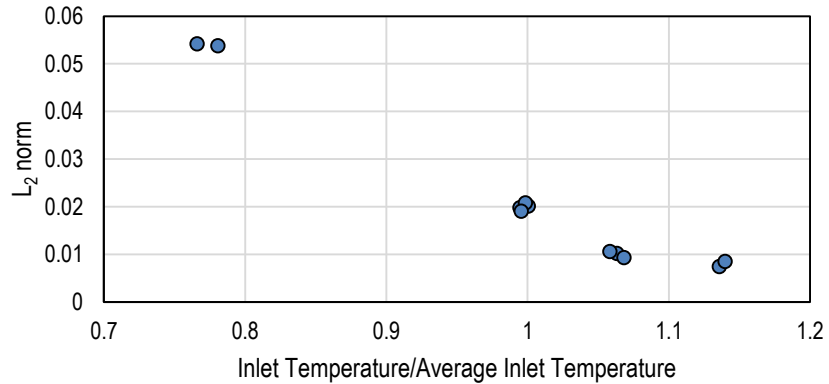
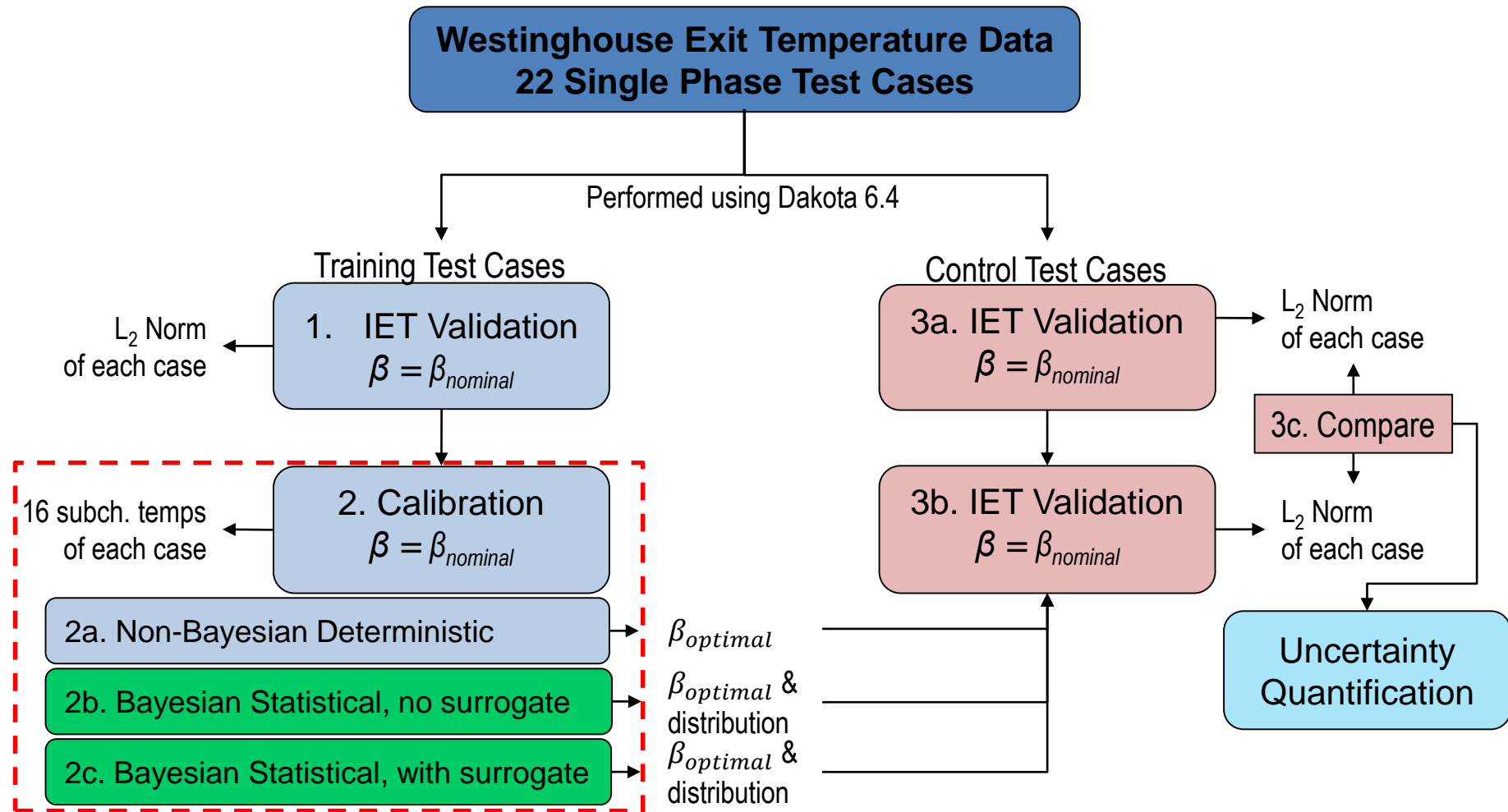


Figure 4

$$L_2 \text{ Norm} = \frac{\sqrt{\sum_1^{36} |CTF_{QOI} - exp_{QOI}|^2}}{\sqrt{\sum_1^{36} |exp_{QOI}|^2}} \quad (1)$$

CTF results at the nominal value of  $\beta$  were validated against the experimental data for half the data (11 test runs), called the training data. All results are representative of only the single phase data provided by WEC. The L<sub>2</sub> norm was used as a metric for determining how close/far away the CTF results were from the experiment (see Equation 1). For most of the test runs, the L<sub>2</sub> norm was within approximately 2% of the experimental data, however two test runs yielded CTF L<sub>2</sub> norms between 5 and 6%.

## 2. Calibration



Calibration is split into three steps, deterministic calibration, Bayesian analysis without a surrogate, and Bayesian analysis with a surrogate (see red dashed box above). The ncsu\_direct method, a derivative-free global optimization method, was used for the deterministic analysis, and Bayesian analysis will be performed using QUESO. Steps 2b and 2c (highlighted in green) are in progress at the end of FY16.

## 2a. Calibration of Training Data

### Non-Bayesian Deterministic Global Calibration

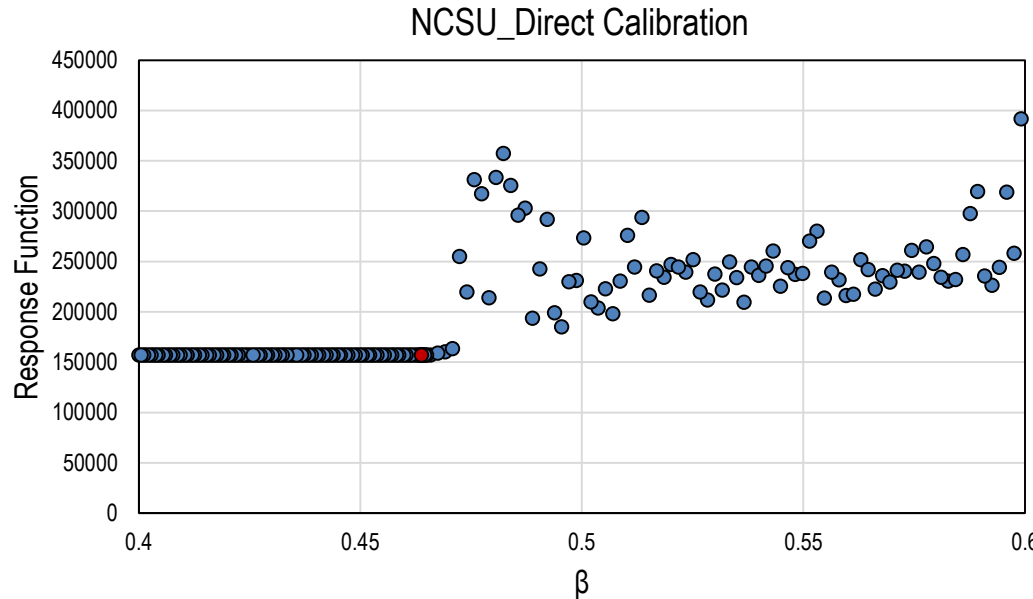


Figure 5

The calibration parameter chosen for CTF Hi2Lo is the constant version of  $\beta$ , the turbulent mixing coefficient. Initially the derivative-based, local calibration method, nl2sol, was chosen for deterministic calibration. It was determined that varying  $\beta$  leads to noise since Dakota would only run 2 evaluations, one at the nominal value and the other at the minimum value before exiting the Dakota run. A derivative-free, global calibration method, ncsu\_direct, was subsequently selected. Figure 5 is the result of the deterministic calibration of  $\beta$ . 401 evaluations were completed for this calibration study and all 36 subchannels were incorporated in this study. The optimal value of  $\beta$  is where the response function value is at a minimum. For this study, the optimal value is 0.464. Note, however that these results will change when the deterministic calibration workflow is modified to calculate the optimal  $\beta$  over only the 16 inner subchannels (explained in Next Steps).

# 2b-c. Calibration of Training Data

## Bayesian Statistical Inference Calibration

Bayesian calibration for CTF is still being investigated and will be performed using the QUESO solver in Dakota 6.4. As with deterministic calibration, constant  $\beta$  is the designated calibration parameter. To ensure that the Bayesian results are not skewed by the outer subchannels in the bundle, only the 16 inner subchannels will be evaluated. Each analysis will take into account the variance in the experimental data.

Bayesian analysis without a surrogate will initiate CTF runs by sampling different  $\beta$  values for each of the experimental test conditions. A new workflow needs to be developed to eliminate the outer subchannel temperatures before passing the results to Dakota.

The Bayesian surrogate work is on hold until a new feature is implemented into Dakota that will take into account the configuration variables (experimental inlet conditions) in addition to the calibration parameter(s) when building a surrogate. Another add-in feature will keep Dakota from re-building the surrogate for each experiment, allowing the user to use one overall surrogate for multiple experiments. In the interim, Dakota LHS studies are being used to collect samples over the entire experimental condition testing range to use for surrogate building once the Dakota modifications are ready. Approximately 1040 samples were generated to build the surrogate.

# CTF Run Time (MV Training Data)

CTF Evaluation	EXP Test Case	Time/Run (min)
1	7	1.961
2	9	2.007
3	11	1.861
4	13	2.073
5	15	1.924
6	17	1.915
7	19	1.970
8	21	1.868
9	23	1.861
10	25	1.883
11	75	1.949
Average Time/Run (min)		1.934

Table 2

To determine if performing Bayesian analysis without a surrogate is computationally reasonable, a small study was performed using the training MV experimental data.

The time splits in Table 2 represent the 11 test runs performed during validation. The third column (Time/Run) is the number of minutes it took CTF to run each test case under the specified test conditions. The average time per CTF run is 1.93 minutes. The relatively short run times mean that CTF can be explicitly calibrated during Bayesian analysis in addition to the generation of a surrogate to model CTF.

# NEXT STEPS

The next step in the CTF Hi2Lo process is Calibration. Deterministic calibration needs to be re-run without the external 20 channels since the thermocouples in these subchannels could be closer or further away from the bundle housing than expected. The Bayesian calibration process without a surrogate also needs to be modified to exclude the outer 20 channels. For the Bayesian calibration process using a surrogate, updates to Dakota's surrogate generation capability need to be made to account for the range in experimental parameters when creating the surrogate.

Since the VMA workshop in July 2016, the sensitivity of CTF subchannel outlet temperatures to the value of  $\beta$  was investigated with comparisons to the experimental data and STAR-CCM+ results. The analyses performed included investigating the distributions of relative percent error between CTF and the experiment for each of the 16 inner subchannels (see following slides). This was performed for an older set of experimental data with non-mixing vane (NMV) grids (test bundle 19) as well as the mixing vane (MV) grid data set (test bundle 20 used previously) to determine if the NMV data set is more sensitive to changes in  $\beta$ .

In addition to studying the temperature distributions at the outlet, it might be of interest to perform the Hi2Lo process on the axial temperature distributions of CTF and STAR-CCM+. While there is not experimental data in the axial direction for validation, a Hi2Lo study could be performed between STAR-CCM+ and CTF.

# Calculating Radial Distance for Plotting

		0.1635	0.577	1.077	1.577	2.077	2.4905	x+
		1 (0.1635,0.1635)	2 (0.577,0.1635)	3 (1.077,0.1635)	4 (1.577,0.1635)	5 (2.077,0.1635)	6 (2.4905,0.1635)	
		7 (0.1635,0.577)	8 (0.577,0.577)	9 (1.077,0.577)	10 (1.577,0.577)	11 (2.077,0.577)	12 (2.4905,0.577)	
		13 (0.1635,1.077)	14 (0.577,1.077)	15 (1.077,1.077)	16 (1.577,1.077)	17 (2.077,1.077)	18 (2.4905,1.077)	
		19 (0.1635,1.577)	20 (0.577,1.577)	21 (1.077,1.577)	22 (1.577,1.577)	23 (2.077,1.577)	24 (2.4905,1.577)	
		25 (0.1635,2.077)	26 (0.577,2.077)	27 (1.077,2.077)	28 (1.577,2.077)	29 (2.077,2.077)	30 (2.4905,2.077)	
		31 (0.1635,2.4905)	32 (0.577,2.4905)	33 (1.077,2.4905)	34 (1.577,2.4905)	35 (2.077,2.4905)	36 (2.4905,2.4905)	

\* All dimensions in inches

★  $x_H, y_H$   
★ (1.327, 1577)

Figure 6

$$R = \sqrt{(x_i - x_H)^2 + (y_i - y_H)^2} \quad (2)$$

Since subchannel plots can be confusing or hard to read, a method for plotting in terms of radial distance from the hottest location within the bundle, or R, was developed (see Figure 6). Coordinates for the center of each subchannel were plugged into Equation (1) to find R. R was then plotted against percent error relative to the experiment for each subchannel and value of  $\beta$  (see following slides).

# Experimental Concerns

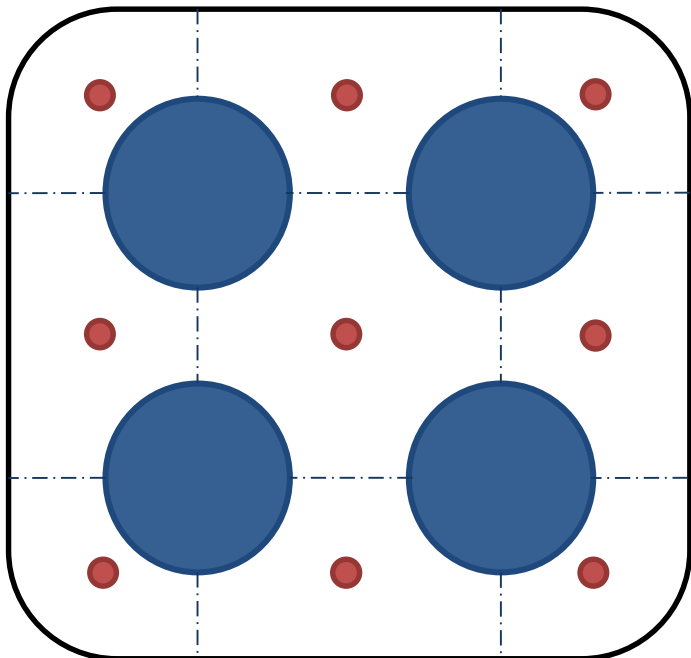


Figure 7

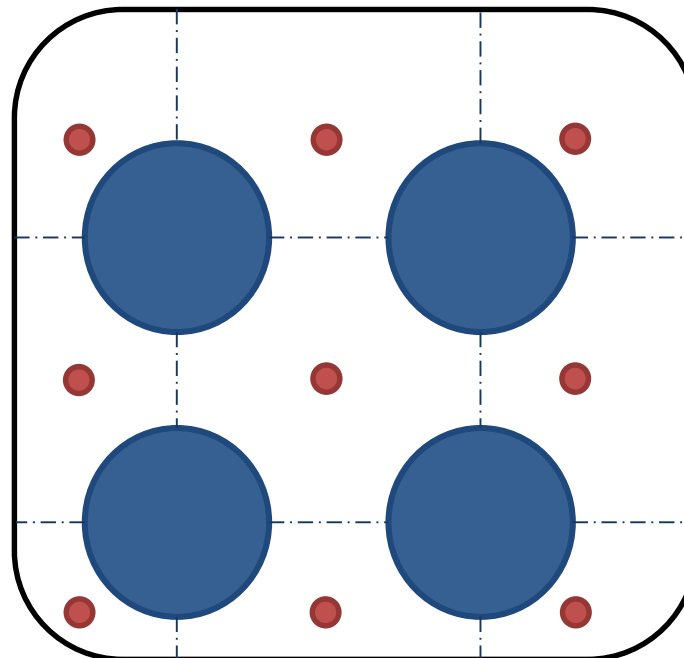


Figure 8

- Location of thermocouples

One concern with the experimental data is that misalignment between the rod bundle and the housing might have occurred between tests. This could change the thermocouple readings in the exterior subchannels in particular since the housing walls could be closer or further away (Figure 8) from the thermocouples than intended (Figure 7). It was the recommendation of the Westinghouse representatives to omit the outer subchannels from analysis since the reliability of the measurement in the outer 20 subchannels is unknown. Note that the bundle shift in Figure 8 is exaggerated for demonstration purposes. The bundle needs only to be slightly misaligned to skew the external thermocouple readings.

# NMV Tout with Different $\beta$ Values

\*Note: No STAR results for this study

NMV Bundle 19 Run 117

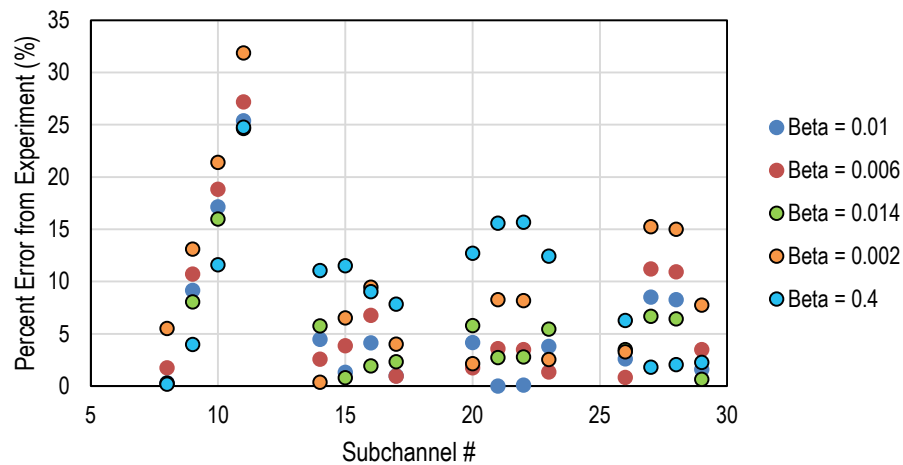


Figure 9

NMV T19 R117

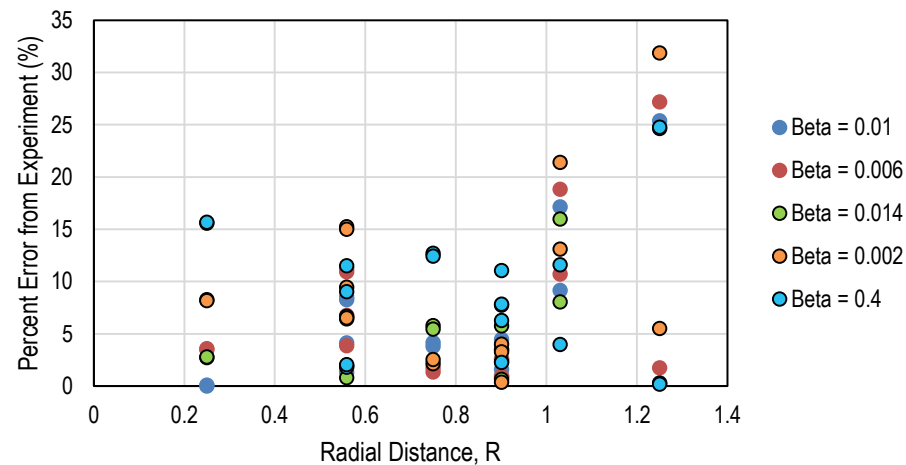


Figure 10

Due to the concern that the bundle was misaligned with the housing during the experiment, the outer subchannels are omitted from all plots in the remainder of this presentation. Percent error was calculated to ensure all results are plotted on the same scale:

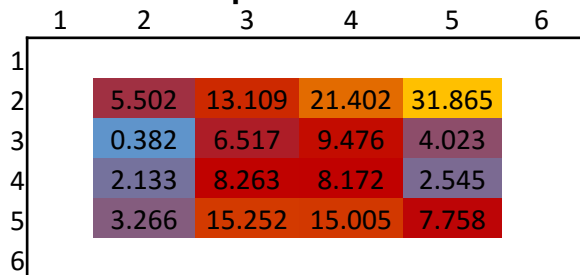
$$\% \text{ error from experiment} = \frac{(T_{CTF,i} - T_{EXP,i})}{(T_{EXP,i} - T_{EXP,inlet})} \times 100 \quad (3)$$

where  $i$  represents each subchannel. Figure 9 is a plot of percent error vs. subchannel number. Since this plot can be more confusing, especially due to the position of the “hot rods”, Figure 10 was generated to plot percent error in terms of distance from the hottest point in the bundle. For the inner 16 subchannels, the largest percent error (deviation from the experiment) is approximately 32% and the lowest is less than 1%.

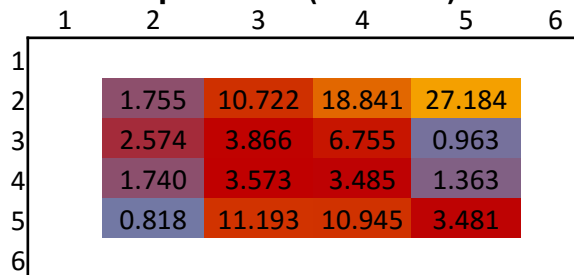
# NMV Test 19 Run 117 Relative % Error

\*Note: No STAR results for this study

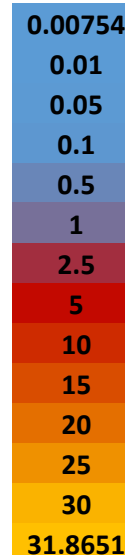
$\beta = 0.002$



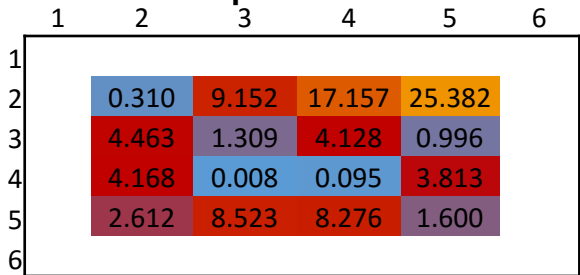
$\beta = 0.006$  (Nominal)



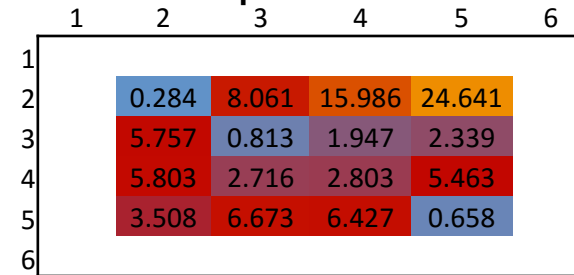
% Error max



$\beta = 0.010$

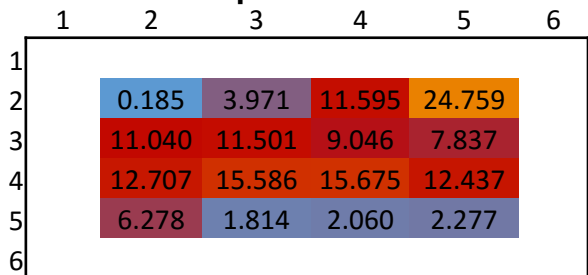


$\beta = 0.014$



% Error min

$\beta = 0.400$



These plots demonstrate the variability in percent error with changes in  $\beta$  as well as the effects of symmetry on the percent error. Differences in symmetry between CTF and the experiment can result in larger percent errors for a particular subchannel.

# MV Tout with Different $\beta$ Values & STAR

MV Bundle 20 Run 7

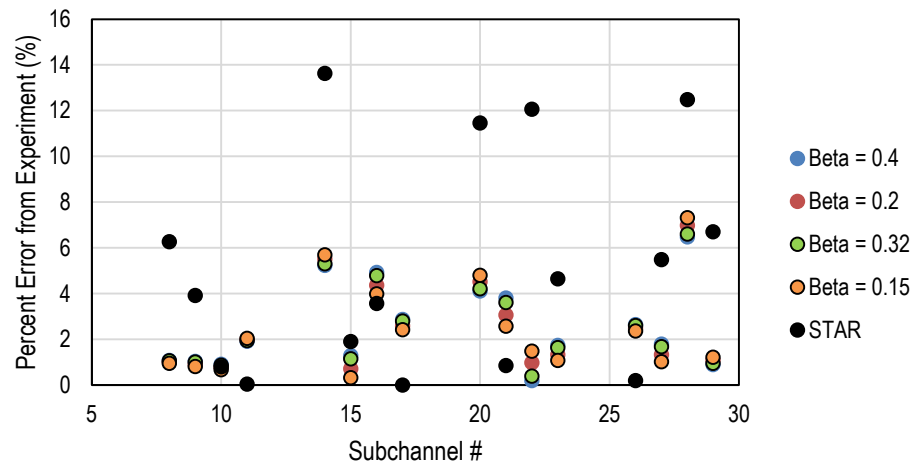


Figure 11

MV Bundle 20 Run 7

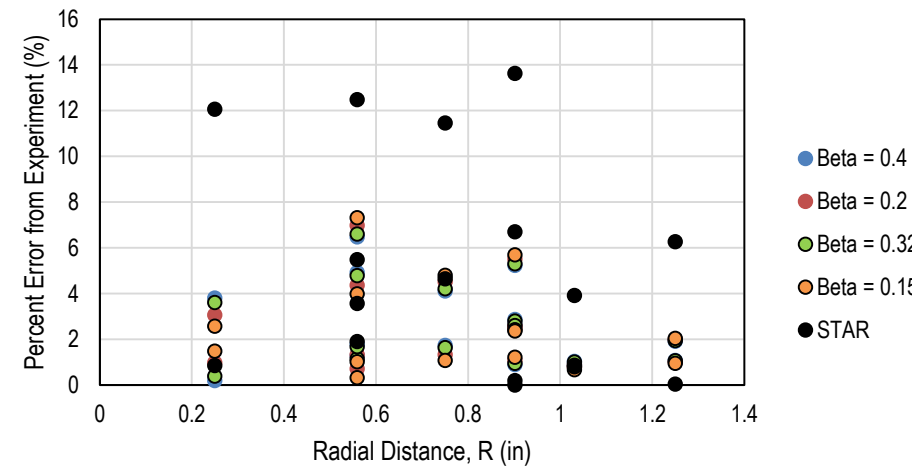
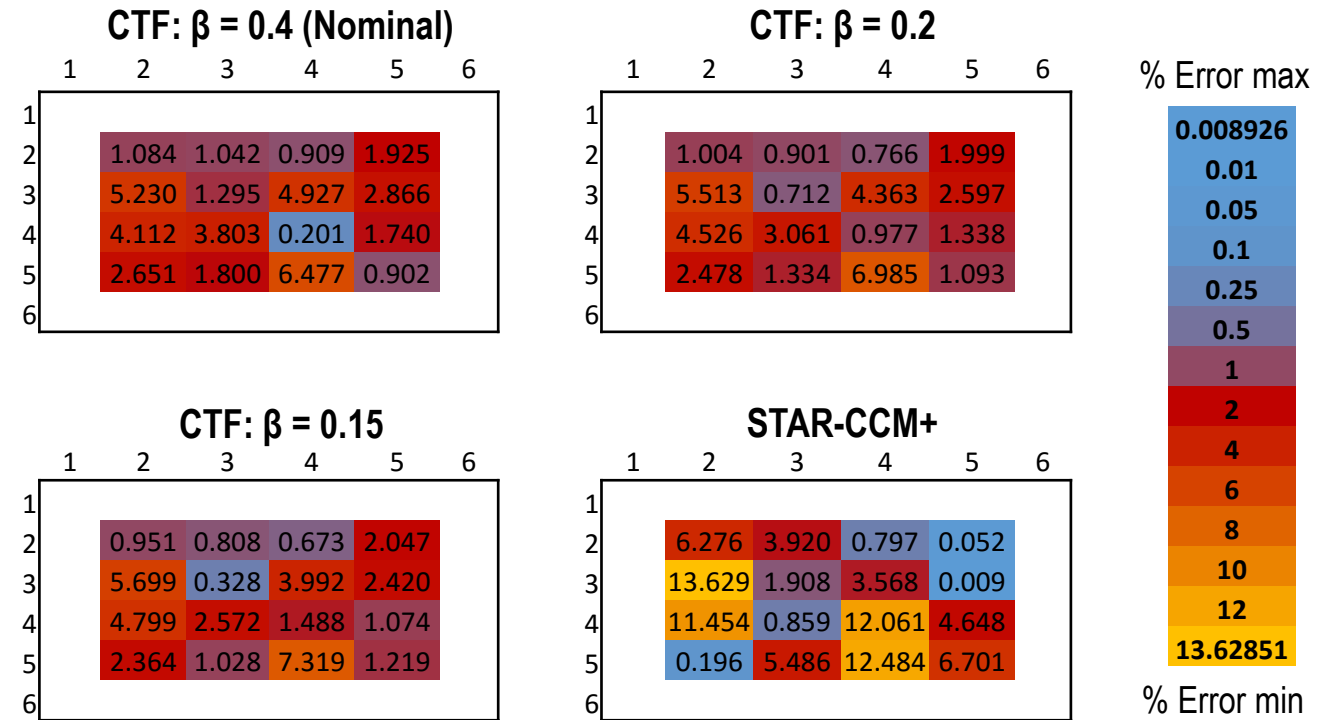


Figure 12

Similarly to the NMV analysis, CTF results with varying values of  $\beta$  were plotted in terms of percent error from the experimental data. For the MV tests, STAR-CCM+ results are available and the same percent error calculations are included in Figures 11 and 12. The plotted values of  $\beta$  yield a maximum percent error of less than 8% and a minimum of approximately 0.2%. The STAR-CCM+ results for the inner 16 channels are somewhere between a minimum percent error of 0.009% or a maximum of approximately 14%. Part of the difference can be attributed to variations in the temperature distribution at the outlet between STAR-CCM+ and the experiment. These plots imply that CTF has greater precision in predicting temperature values closer to the experiment than STAR-CCM+.

# MV Test 20 Run 7 Relative % Error



As mentioned previously, differences in temperature distributions, especially the symmetry at the outlet, between the experiment and STAR-CCM+/CTF can impact the percent error significantly. It is more apparent in the distribution plots above that while STAR-CCM+ predicts temperatures closer to the experimental measurements than CTF for some subchannels, it also predicts temperatures further away than CTF for other subchannels even when the outer subchannels are neglected from the analysis. Additionally, as expected with the MV CTF runs around a nominal value of  $\beta$ , the percent error distribution is more uniform.

# Potential Path: Axial Temperature

MV T20 R7 SC22

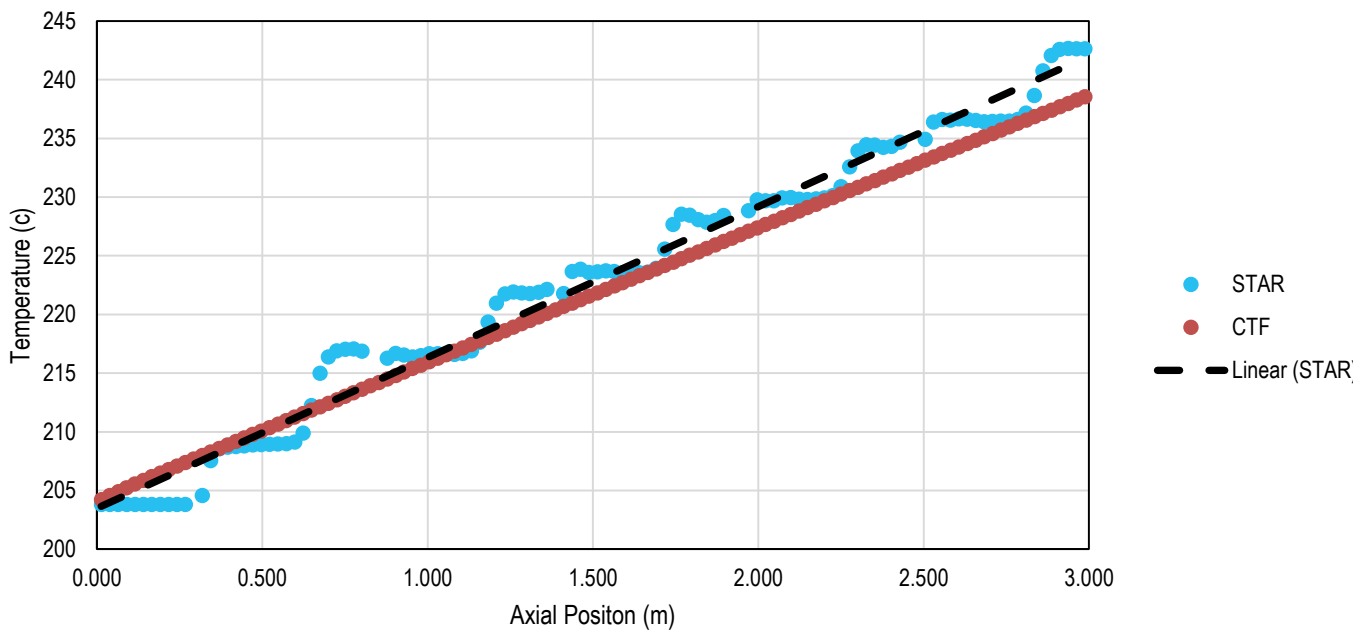
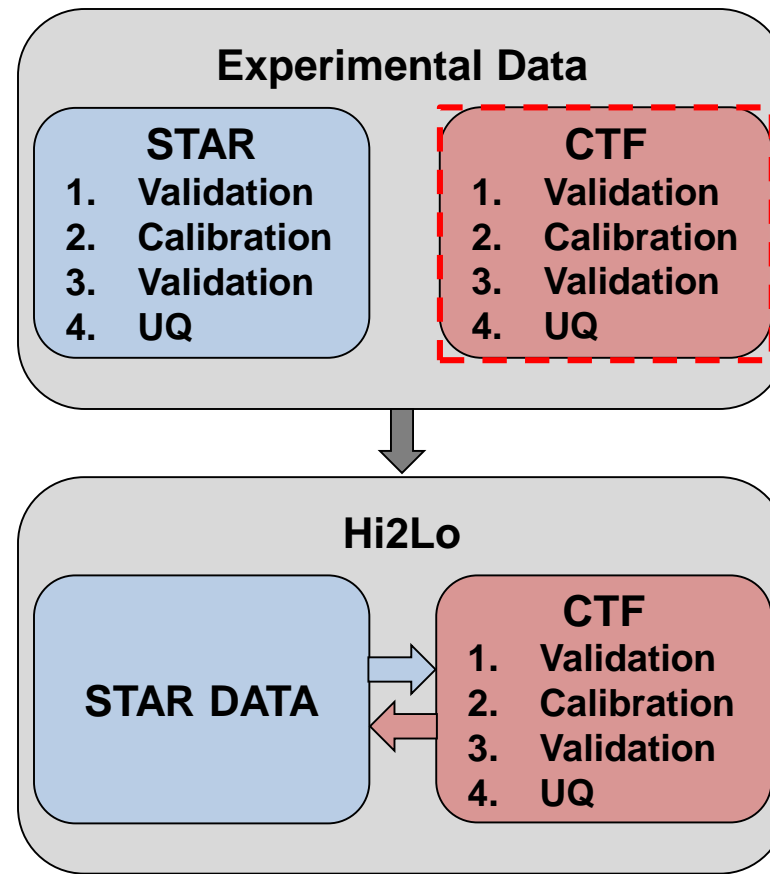


Figure 13

The hot channel (SC22) axial temperatures were selected to compare between STAR-CCM+ and CTF. While CTF does not model the grids explicitly, the temperature profile is expected to exhibit a step-wise pattern, however the results from CTF are a straight line. The STAR-CCM+ results follow the characteristic stair-step pattern. Interestingly, a trendline of the STAR-CCM+ results closely matches CTF until approximately 1.5 m downstream of the bundle inlet. STAR-CCM+ then produces higher temperatures for the second half of the bundle. This might be interesting to pursue for the 16 inner subchannels.

# Hi2Lo Introduction

## Hi2Lo Workflow



The CTF box highlighted in dashed red represents the current phase of the Hi2Lo process. In parallel, STAR-CCM+ is going through the same process and both utilize experimental data to benchmark the analysis. The next phase of the process is to use STAR-CCM+ in place of the experimental data since it is difficult to obtain detailed experimental data.